

PDF hosted at the Radboud Repository of the Radboud University Nijmegen

The following full text is a preprint version which may differ from the publisher's version.

For additional information about this publication click this link.

<http://hdl.handle.net/2066/92024>

Please be advised that this information was generated on 2018-07-08 and may be subject to change.

Magnetoelastic coupling in γ -iron

S. V. Okatov

Institute of Quantum Material Science, 620107, Ekaterinburg, Russia

Yu. N. Gornostyrev

*Institute of Metal Physics, Russian Academy of Sciences, Ural Division, Ekaterinburg, 620219 and
Institute of Quantum Material Science, 620107, Ekaterinburg, Russia*

A. I. Lichtenstein

Institut für Theoretische Physik, Universität Hamburg, Jungiusstrasse 9, 20355, Hamburg, Germany

M. I. Katsnelson

Radboud University Nijmegen, Institute for Molecules and Materials, 6525AJ, Nijmegen, the Netherlands

Exchange interactions in α - and γ -Fe are investigated within an *ab-initio* spin spiral approach. We have performed total energy calculations for different magnetic structures as a function of lattice distortions, related with various cell volumes and the Bain tetragonal deformations. The effective exchange parameters in γ -Fe are very sensitive to the lattice distortions, leading to the ferromagnetic ground state for the tetragonal deformation or increase of the volume cell. At the same time, the magnetic-structure-independent part of the total energy changes very slowly with the tetragonal deformations. The computational results demonstrate a strong mutual dependence of crystal and magnetic structures in Fe and explain the observable “anti-Invar” behavior of thermal expansion coefficient in γ -Fe.

PACS numbers: 75.50.Bb, 71.15.Nc, 75.30.Et, 75.30.Ds, 65.40.De

Keywords:

I. INTRODUCTION

Iron-based alloys are still among the most important industrial materials. The thermodynamic properties and mechanism of phase transformations in these materials have been discussed intensively last years¹. Nevertheless, the fundamental properties of iron have not been completely understood up to now. Main difficulties are related with a non-trivial combination of the itinerant and localized behavior and correlation effects of $3d$ -electrons determining electronic, magnetic and structural properties of iron²⁻⁶. It is commonly accepted now that magnetic degrees of freedom play a crucial role in the stability of different iron phases⁷⁻¹⁰ which makes the situation even more complicated. Interplay between magnetic and lattice degrees of freedom in different crystallographic phases of iron remains still unresolved problem.

One of the most complicated example related γ -phase of iron with highly frustrated magnetic structure. There are many magnetic configurations of γ -Fe with almost the same total energies and the ground state is crucially depends on the value of lattice parameters¹¹⁻¹³. The sensitivity to dilatation has been studied in detail by many groups¹⁴⁻¹⁶ in the context of a so called moment-volume instability¹⁷. At the same time, the energy dependence on the tetragonal deformation which is closely related with the Bain deformation path of $\alpha - \gamma$ phase transformation also deserves a serious attention. We discussed this issue in our previous work¹⁸ and found that the transition of γ -Fe to the ferromagnetic state can trigger the martensitic transformation without noticeable energy

barriers. In more detail, the effect of tetragonal deformations on magnetism and vice versa was discussed in relation with the Invar behavior observed in Fe-Ni alloys^{17,19}. A magnetoelastic spin-lattice coupling plays also an important role in structural phase transitions in γ -Mn²⁰ and Cr-based alloys²¹, as well as in the magnetic shape-memory alloy Ni₂MnGa²². A soft-mode phonon behavior, as a precursor of the $\gamma \rightarrow \alpha$ transformation, was recently observed in Fe-Ni alloys²³.

In contrast with Fe-Ni alloys, the equilibrium γ -phase in pure Fe exists only at high temperatures $T > 1200$ K where thermal fluctuations are very strong and magnetic moments are disordered. Observation of the so-called “anti-Invar” behavior of γ -Fe²⁴ can be related with the fact that the spin-lattice coupling is strong enough to affects the thermodynamic properties up to very high temperatures.

In this paper we investigate quantitatively a variation of the exchange parameters in α - and γ -Fe as functions of tetragonal Bain-deformations and dilatation. Whereas the sensitivity of the exchange parameters to the dilatation has been studied previously¹⁴⁻¹⁶ an information about the tetragonal deformations have been missing until now. Based on the calculated magnetic exchange data we discuss the origin of the anti-Invar behavior of γ -Fe.

II. COMPUTATIONAL APPROACH

The standard approach to study magnetic properties of itinerant-electron transition-metal systems related with

the mapping of density functional total energies on the effective classical Heisenberg model:

$$H_{ex} = - \sum_{i < j} J_{i,j} \mathbf{e}_i \mathbf{e}_j \quad (1)$$

where \mathbf{e}_i is the unit vector in direction of the magnetic moment at site i ^{25,26}. In this notation the value of on-site atomic magnetic moments M_i is included into the exchange parameters $J_{i,j}$. Therefore the total energy of the system is a sum of a magnetic-structure independent contribution E_0 and the ‘‘Heisenberg-exchange’’ part: $E = E_0 + H_{ex}$, where E_0 is a function of deformations and the magnitude of local moments: $E_0(\Omega, c/a, M)$. A similar decomposition was used earlier in Ref. 27. One should stress that E_0 is dependent on the values of magnetic moments M_i and is therefore essentially different from the energy of a non-spin-polarized state, which attribute is zero all magnetic moments: $M_i = 0$.

There are two main approaches to the mapping onto magnetic Hamiltonian. An analytical scheme is based on the use of so-called ‘‘magnetic force theorem’’^{25,26}, when the exchange interactions are obtained from variations of the total energy with respect to infinitesimal deviations of the magnetic moments from a collinear state. In this paper we use more accurate numerical method based on the density functional calculations of the spin spiral magnetic structures where the neighboring magnetic moments are rotated relative to each other by a finite angle (for review, see Ref. 28). This scheme includes a spin- and charge-density relaxation for large moment fluctuations. The energy per atom of the spin spiral with the wave vector \mathbf{Q} can be presented as:

$$\begin{aligned} E(\mathbf{Q}) &= E_0 - \frac{1}{N} \sum_{i < j} J_{i,j} \exp(i\mathbf{Q} \cdot \mathbf{R}_{i,j}) \\ &= E_0 - \sum_n Z_n J_n \exp(i\mathbf{Q} \cdot \mathbf{R}_n), \end{aligned} \quad (2)$$

where N is the number of magnetic atoms, Z_n is the number of the n -th nearest neighbor atoms, E_0 is a magnetic-structure-independent contribution to the total energy of the system, $\mathbf{R}_{i,j}$ is the vector connecting sites i and j , n labels the coordination shell. The exchange parameters J_n can be found from Eq. (2) by using the discrete Fourier transformation:

$$J_n = -\frac{1}{K} \sum_k E(\mathbf{Q}_k) \exp(i\mathbf{Q}_k \cdot \mathbf{R}_n), \quad (3)$$

where the summation runs over a regular \mathbf{Q} -vector mesh in Brillouin zone with the total number of points K . As follows from Eq.(3) the value E_0 is the average value of spin spiral energies over all \mathbf{Q}_k ,

$$E_0 = \frac{1}{K} \sum_k E(\mathbf{Q}_k). \quad (4)$$

In principle, one can find the dependence of total energy on magnitude of M within a constrained moment spin-spiral calculations, but this lay beyond a scope of present

paper. A parameter of total exchange energy

$$J_0 = \sum_n Z_n J_n \quad (5)$$

characterizes a ferromagnetic contribution to the total energy. Note that the decomposition of the total energy used in Ref. 27 differs from that used in this work by a shift by J_0 .

In general, the exchange parameters found from the planar spin spiral calculations and from the magnetic force theorem are different and only the value of a spin stiffness constant should be the same²⁹. Note that parameters obtained by the use of infinitesimal spin deviations^{25,26} give a correct description of a magnon spectra, while parameters found from a direct calculation of the spin spiral total energies are supposed to be more accurate for descriptions of thermodynamic properties²⁹. The difference of J_n obtained within these two approaches characterizes a non-Heisenberg character of magnetic interactions which is expected for itinerant magnets such as iron³⁰. Another manifestation of the non-Heisenberg behavior related with the fact that the magnitude of the magnetic moments dependent on the spin spiral wave vector \mathbf{Q} . Therefore, the values J_n obtained in the framework of spin spiral approach are considered as *effective* exchange parameters.

The total energy calculations of Fe with spin spirals magnetic structure is performed using VASP (Vienna Ab-initio Simulation Package)³¹⁻³³ with first-principle pseudopotentials constructed by the projected augmented wave method (PAW)³⁴. Following an experience on non-collinear magnetic investigation¹³ we employed the generalized gradient approximation (GGA) for the density functional in a form by Perdew and Wang (1991)³⁵ with the spin-interpolation³⁶. The PAW potential without core states and with energy mesh cutoff 530 eV, and the uniform k -point $12 \times 12 \times 12$ mesh in the Monkhorst-Park scheme³⁷ with 1728 k -points are used. The calculations are done for a single-atom unit cell subjected by two types homogeneous deformations, namely, dilatation (a change of the volume for a fixed c/a ratio) and tetragonal ones (a change of c/a ratio at a fixed volume). For given lattice parameters, the energy set $E(\mathbf{Q}_k)$ is calculated on a uniform $16 \times 16 \times 16$ mesh and the Fourier transformation (Eq. 3) is used to determine the exchange parameters J_n .

III. COMPUTATIONAL RESULTS

The local magnetic moments $M(\mathbf{Q})$ and total energies for the spin spiral states $E(\mathbf{Q})$, calculated for different values of volume and tetragonal deformations are presented in Figs. 1 and 2, respectively. We show the results only for the symmetric directions of the wave vector $\Gamma - Z - W(U)$ in Brillouin zone parallel to $\langle 001 \rangle$ and $\langle 012 \rangle$ in lattice with cubic (tetragonal) symmetry¹³.

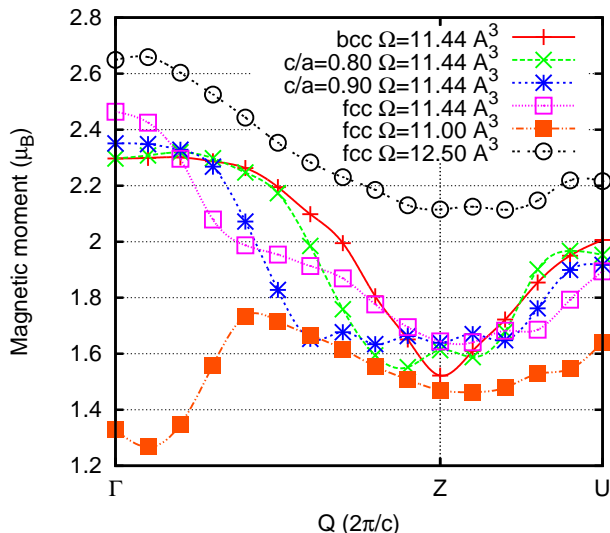


FIG. 1: (Color online) The magnetic moment of iron as function of the spin spiral vector \mathbf{Q} and the lattice deformations.

The magnetic moments depend strongly on the spin spiral wave vector \mathbf{Q} , as one can see from Fig. 1. This fact confirms the non-Heisenberg character of magnetic interactions in iron. The magnitude of magnetic moments gradually decrease by about 30% along $\Gamma - Z$ direction for all considered structures except for fcc iron at small volume $\Omega = 11.0 \text{ \AA}^3$. Large difference of magnetic moments for fcc Fe at Γ -point at a small volume ($\Omega = 11.0 \text{ \AA}^3$) and bigger ones ($\Omega \geq 11.44 \text{ \AA}^3$) results from a well known magnetovolume instability which was discussed in the context of the Invar problem¹⁷.

According to our results (Fig. 2) the ground state of fcc iron is spin spiral with \mathbf{Q} varying nearby $0.5\langle 001 \rangle$ (in $2\pi/c$ units) with volume and c/a ratio for a broad interval $10.5 < \Omega < 12.0 \text{ \AA}^3$. The magnetic ground state of fcc iron is a controversial issue up to now. The antiferromagnetic double layer structure (AFMD), equivalent the spin spiral with $0.5\langle 001 \rangle$ has been discussed in a series of papers^{11,48,49}. The later publications^{13,14,51} show, rather incommensurate ground states with \mathbf{Q} -vector depending on lattice parameters. Our result are in agreement with the recent calculations^{13,14,38,39,47,51}.

An increase of iron volume further $\Omega > 12.0 \text{ \AA}^3$ results in the transition from spin spiral to ferromagnetic (FM) structure (Fig. 2a). The energy difference ΔE_M between FM and antiferromagnetic (AFM) states (or spin spiral structure with $\mathbf{Q} = \langle 001 \rangle$) gives a scale of the exchange interaction energy which decreases monotonously with increasing of the volume and finally changes the sign near $\Omega_{\text{exp}} = 11.44 \text{ \AA}^3$. This volume corresponds to an experimental value for precipitates of γ -Fe in Cu at low temperatures⁵⁰.

Our results demonstrate that the magnetic structure of fcc iron is strongly dependent on the lattice deformations (Fig. 2). This conclusion agrees well with the previous

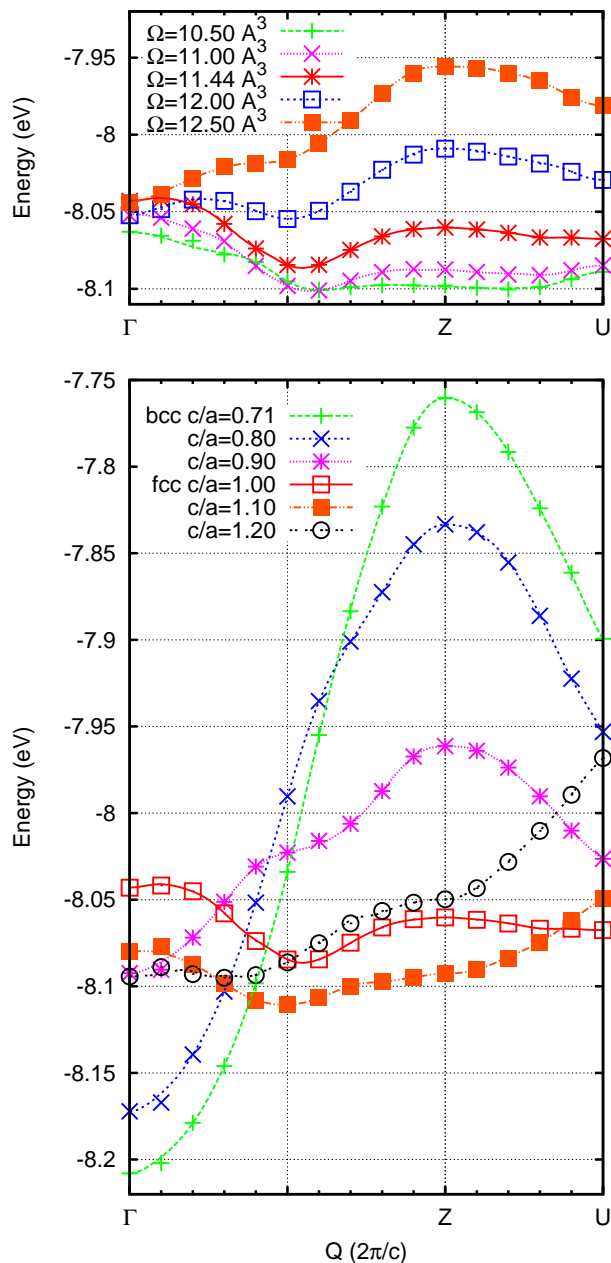


FIG. 2: (Color online) Dependence of the total energy of fcc Fe on the the spin spiral wave vector $E(\mathbf{Q})$ for different volumes (upper panel, $c/a=1$) and for different c/a ratios (lower panel, $\Omega=11.44 \text{ \AA}^3$). The deformations $c/a = 1/\sqrt{2}$ and $c/a = 1$ correspond to the bcc (α -Fe) and fcc (γ -Fe) structures, respectively. Symbols mark the results of the density functional calculations whereas the lines correspond Eq. (2) with obtained exchange parameters J_n .

investigations of iron^{13,18,51}. In particular, the spin spiral ground state is changed to the ferromagnetic one within the tetragonal deformation region along the Bain path from the fcc ($c/a = 1$) to bcc iron ($c/a = 1/\sqrt{2}$). A magnetic transition to the FM state and its role in the martensitic transformation have been discussed earlier in

Ref. 18. In the opposite case, when $c/a > 1$, the tetragonal deformation leads to a weaker dependence of $E(\mathbf{Q})$. The spin spiral structure represents a ground state at $c/a \approx 1.1$ and a transition to the ferromagnetic ground state appeared at $c/a \geq 1.2$. This magnetic transformations are in agreement with a previously obtained phase diagram⁵¹.

The results for exchange parameters $J_n(c/a, \Omega)$ as function of lattice distortions are presented in Fig. 3. Positive values indicate that the ferromagnetic type of ordering is preferable. The dependence $E(\mathbf{Q})$ determined by Eq. (2) with obtained exchange parameters J_n give a perfect interpolation to the calculated spin spiral energies (lines and symbols in Fig. 2). A striking feature of this curves is that the total exchange energy J_0 behaves similar to $Z_1 J_1$ (Z_i corresponds to number of i -th neighbors) for all deformations considered. This means that the contributions of longer-range exchange interactions ($n > 1$) are canceled out. Similar results have been obtained by analytical calculations of exchange parameters¹⁶ for the volume variation of fcc iron.

Effects of volume variation on the exchange parameters in fcc structure is very noticeable and J_1 demonstrates there a non-monotonous behavior (Fig. 3a). At low volumes ($\Omega < \Omega_{\text{exp}}$) total exchange parameter J_0 become negative showing the tendency to antiferromagnetic-type coupling. For atomic volumes near Ω_{exp} the parameter J_1 is close to zero and the exchange energy J_0 is small and negative. In this case the value J_0 is determined by all exchange parameters J_n with $n > 1$. Therefore, computational results for $\Omega \approx \Omega_{\text{exp}}$ appear to be quite sensitive to the details of the approximation used¹⁴ (e.g. the exchange-correlation functional, energy cut-off, number of k-points, etc.). Such behavior of exchange parameters can likely be related to a complex magnetic structure discussed in the experimental work by Tsunoda and co-workers⁵⁰.

Parameter J_0 changes the sign at a volume which is just slightly above the Ω_{exp} and grows rapidly, therefore the ferromagnetic order becomes more stable for higher volumes (Fig. 3a). The behavior of J_0 (Fig. 2) agree well with previous calculations^{15,16} and reproduces the transition from spin spiral to ferromagnetic state discussed above.

In the bcc Fe exchange parameters demonstrate a rather weak sensitivity to the volume variation and the nearest neighbor contribution J_1 is large, positive and dominant in a broad interval of Ω (Fig. 3b). As a result, the ferromagnetic ground state has an essential preference in bcc Fe in comparison with the AFM and non-collinear magnetic structures. Results of previous calculations^{26,39-46} give slightly lower values J_0 and J_1 in bcc Fe than obtained here but also reproduce a dominant contribution of J_1 to the exchange energy.

A dependence of exchange parameters on the tetragonal deformation c/a is presented in the Fig. 3(c,d). A symmetry break caused by tetragonal deformations leads to a modification of the coordination numbers in fcc or

bcc lattice. Here we neglect the rearrangement of site positions and assume that the set of atoms belongs to the same coordination shells n in fcc and fct structures for $0.85 \leq c/a \leq 1.2$ and in bcc and bct structures for $0.6 \leq c/a < 0.85$. The curves $J_1(c/a)$ and $J_0(c/a)$ have both a minima for fcc and a maxima for the bcc structures. One can see that near the bcc structure J_0 is much less sensitive to the dilatation than to the tetragonal deformation. Near the fcc, J_0 is very sensitive to both types of deformations. This is mainly due to sensitivity of J_1 to deformations whereas J_n for $n > 1$ are almost unchanged with variation of lattice parameters.

The dependence of the exchange parameters on both types of deformations is shown in Fig. 4 as a contour plot $J_0(\Omega, c/a)$. One can see that the tetragonal deformation together with the increase in volume enhance significantly the exchange interaction energy in γ -Fe. The value $J_0 \approx 70$ meV is reached for the experimental volume of γ -Fe $\Omega \approx 12 \text{ \AA}^3$ and $(c/a - 1) \approx 5\%$.

Calculated exchange parameters J_n are presented in the Fig. 5 as functions of interatomic distances. The exchange interactions in fcc iron have a very long-ranged behavior at the volumes $\Omega \approx \Omega_{\text{exp}}$. Such a strong Friedel oscillations was already found in Ref. 16. This is a reason of magnetic frustrations and existence of numerous complex magnetic structures with low energies in the fcc Fe^{12,16,38,50}. A tetragonal deformation of the fcc structure changes dramatically the behavior of J_n due to a sharp increase of J_1 contribution which becomes a dominant one. The increase of volume acts in a similar way. One can see from Fig. 5 that the exchange interactions depends not only on interatomic distance R_n but also very sensitive to particular values of c/a . Therefore, correct lattice deformations should be necessarily taken into account *explicitly* for a correct description of magnetic structures in Fe.

IV. DISCUSSION AND CONCLUSIONS

We can determine the magnetic-structure independent contribution E_0 by subtracting the Heisenberg-like contribution with calculated exchange parameters from the total energy. In order to do this one can use the energy of ferromagnetic state in the spin-spiral framework $Q = 0$ from the Eq. (2) and the following expression: $E_0 = E_{\text{FM}} - J_0$. As was mentioned earlier, E_0 essentially differs from a total energy obtained in the non-spin-polarized calculations because of implicit dependence of E_0 on the magnetic moment M . They are equal only for the systems with zero magnetic moments of all atoms.

The results for E_0 are shown in Fig. 6 together with the total energies of FM bcc and FM, AFM and AFMD fcc states obtained by the reconstruction from E_0 and J_n . For comparison, the total energies of E_{NM} obtained from calculations by VASP are also shown. These results agree very well with the previous *ab-initio* calculations⁴⁹ and demonstrate the dramatic difference between E_0 (see

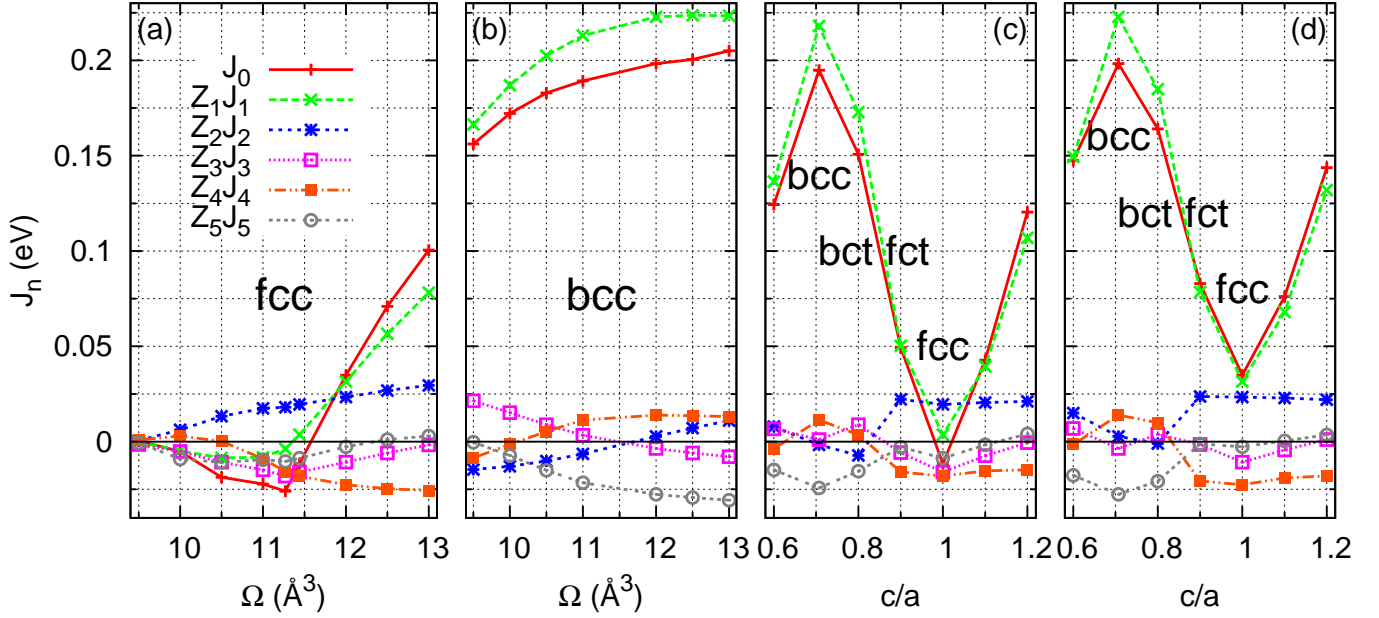


FIG. 3: (Color online) Exchange parameters J_n for $n = 1, 2, 3, 4, 5$ for different lattice parameters: dependence J_n on a volume of fcc (a) and bcc (b) Fe; dependence J_n on (c/a) at fixed volumes $\Omega = 11.44 \text{ \AA}^3$ (c) and $\Omega = 12.0 \text{ \AA}^3$ (d), respectively.

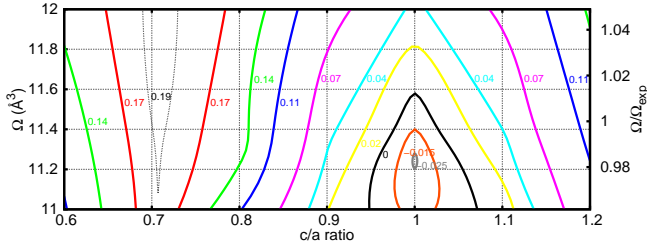


FIG. 4: (Color online) Dependence of the total exchange parameter J_0 on volume Ω and c/a ratio as a contour plot $J_0(\Omega, c/a)$.

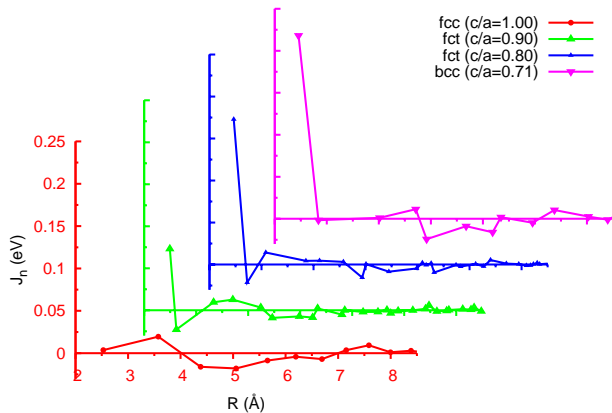


FIG. 5: (Color online) The exchange parameter as a function of interatomic distance to the n -th neighbour $J_n(R_n)$ for different c/a ratios.

Eq. 4) and E_{NM} .

For fcc iron the magnetic-structure independent contribution E_0 is rather close to the energy of AFM and AFMD states. For bcc iron the difference between E_0 and ground-state energy E_{FM} is larger but rather weakly volume dependent compare to fcc states. At the same time, the energy of FM fcc state shows two minima at low and high volumes. This behavior of fcc total energy drastically differs from the E_0 curve. The difference is larger for higher volumes and has entirely magnetic origin due to increase of the exchange parameters with Ω (Fig. 3). Quantitatively, the values of bulk modulus for fcc iron obtained from the Birch-Murnaghan equation of state⁵² for E_0 and E_{AFMD} , E_{AFM} curves differ by about 17% and 30% (161, 189, and 207 GPa, respectively). For the bcc iron estimation of bulk modulus from E_0 and E_{FM} curves give the same $B \approx 187$ GPa, in agreement with the experiment⁵³.

The situation with tetragonal deformations is quite unusual. One can see in Fig. 6b that E_0 depends on c/a very weakly. This means that the Heisenberg-like contribution is dominant in the shear modulus C' , as well as in the whole energy curve along the Bain path. This is main origin of anomalously strong coupling between the magnetic and lattice degrees of freedom in iron, where the tetragonal deformation plays a special role. The curve $E_0(c/a)$ has a minimum at $c/a = 1$ (fcc structure) whereas both E_{FM} and E_{AFMD} have no minima at this point which means instability of fcc phase in both magnetic structures. The minima correspond to bcc (FM) and fct (AFM, AFMD) states with $c/a > 1$.

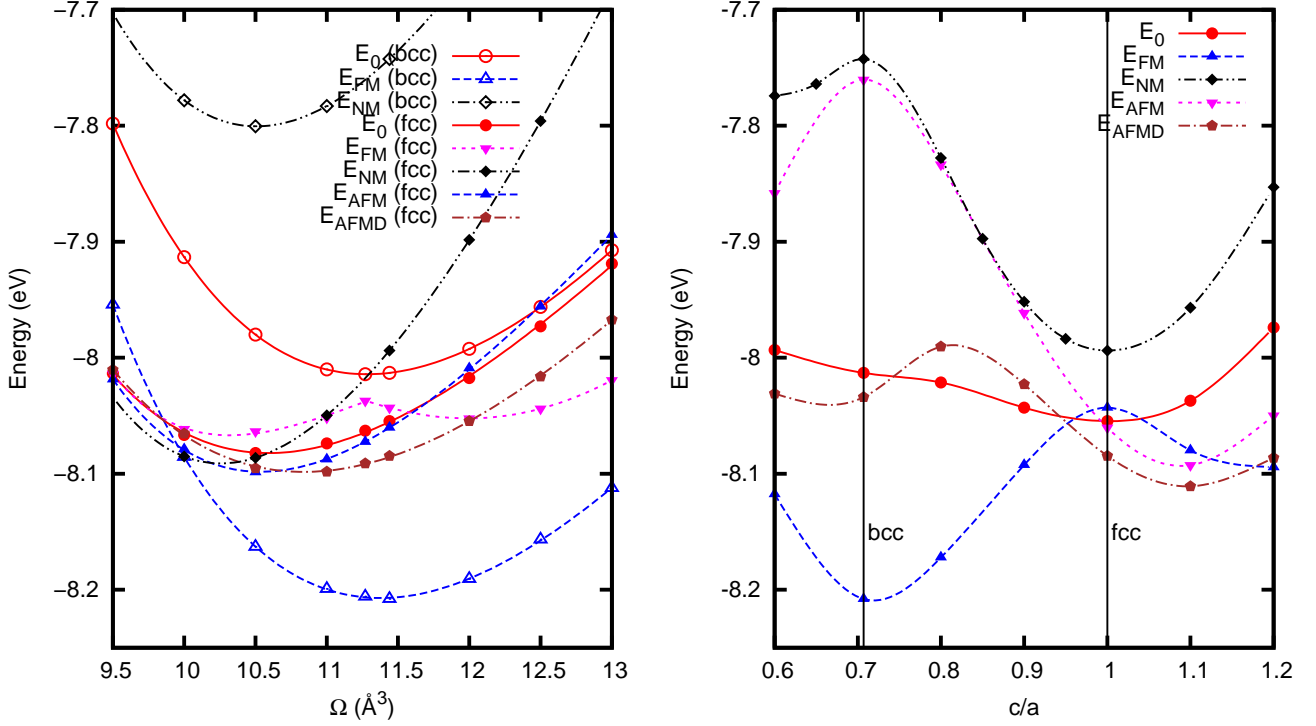


FIG. 6: (Color online) Total energy of iron reconstructed from the E_0 and J_n parameters (symbols) as a function of volume (a) and tetragonal deformation (b) for FM and AFM magnetic structures, as well as the magnetic-structure-independent contribution E_0 to the total energies. The lines are total energy fitting using Birch-Murnaghan equation of state⁵² for (a) and splines for (b). Fitting for the FM state in fcc structure (a) is done separately for each minimum.

Our calculations reveal another unusual feature of the magnetic interactions in fcc iron related with a growth of the exchange parameter J_1 and, as a consequence, J_0 with the volume increase at $\Omega > \Omega_{\text{exp}}$ (see Fig. 3a). This behavior corresponds to the rising branch of the Bethe-Slater curve $J(\Omega)$ which have been used for a semi-quantitative interpretation of the Invar anomaly⁵⁴. This region of volumes corresponds to observed high-temperature phase of γ -Fe; for further increase of interatomic distances the overlap of d -orbitals becomes weaker and the exchange interactions J_n decreases.

Here we show that the calculated dependence of $J_n(\Omega)$ can explain the anti-Invar phenomenon in γ -Fe²⁴. If a magnetic subsystem is well described by the Heisenberg-like model (1) its contribution to pressure according to the Hellman-Feynman theorem is

$$P_m = -\frac{1}{N} \left\langle \frac{\partial H_{ex}}{\partial \Omega} \right\rangle = \frac{1}{N} \sum_{i<j} \frac{\partial J_{i,j}}{\partial \Omega} \langle \mathbf{e}_i \mathbf{e}_j \rangle \approx Z_1 \frac{\partial J_1}{\partial \Omega} \langle \mathbf{e}_0 \mathbf{e}_1 \rangle \quad (6)$$

where Z_1 is the number of nearest neighbors. We assume that the nearest-neighbor interaction is the strongest one which is supported by our first-principle calculations. For a purpose of qualitative discussions, we will treat exchange interactions perturbatively assuming $Z_1 J_1 \ll T$

(T is the temperature and $k_B = 1$). Then one has $\langle \mathbf{e}_0 \mathbf{e}_1 \rangle \approx J_1/3T$ and therefore

$$P_m = \frac{Z_1}{6T} \frac{\partial J_1^2}{\partial \Omega} \quad (7)$$

This means that the pressure induced by magnetic exchange interactions is positive and decreases with the temperature increase.

The thermal expansion coefficient

$$\alpha = \frac{1}{\Omega} \left(\frac{\partial \Omega}{\partial T} \right)_P = \left(\frac{1}{B} \right)_T \left(\frac{\partial P}{\partial T} \right)_\Omega \quad (8)$$

can be divided into magnetic-structure independent part (α_0) and one related with magnetic exchange interactions (α_m): $\alpha = \alpha_0 + \alpha_m$. The magnetic exchange part is equal to

$$\alpha_m = \frac{1}{B} \left(\frac{\partial P_m}{\partial T} - B_m \alpha_0 \right) \quad (9)$$

Here B is isothermal bulk modulus $B = B_0 + B_m$, B_0 is the magnetic-structure independent part of B , and $B_m = -\Omega(\partial P_m/\partial \Omega)_T$. Usually, the second term in Eq.(9) is neglected. Since $\partial P_m/\partial T < 0$ one can assume that the expression (7) should lead to the Invar behavior, and hence to the negative contribution to the thermal expansion coefficient. A strong volume dependence of the

exchange parameter J_1 can lead to the opposite conclusion. Substitutes Eq. (7) into Eq. (9) one finds

$$\alpha_m = -\frac{1}{B_0} \frac{Z_1}{6T} \frac{\partial J_1^2}{\partial \Omega} \left[1 - \alpha_0 T \frac{\partial \ln(\partial J_1^2 / \partial \Omega)}{\partial \ln \Omega} \right] \quad (10)$$

Using calculated volume dependence $J_1(\Omega)$ (Fig. 3) and values α_0, Ω obtained from the experiment²⁴ one can find that the second term in square brackets in the right-hand side of Eq. (10) is approximately 1.1 at the temperature of 1200 K. Therefore, a total magnetic exchange contribution to the thermal expansion coefficient (10) has *positive* sign. This corresponds to the *anti*-Invar behavior, in a qualitative agreement with the experimental data²⁴.

The negative magnetic exchange contribution to the thermal expansion coefficient α_m in the Invar materials usually is associated with a thermal dependence of the spontaneous magnetostriction¹⁹, while the positive contribution (anti-Invar behavior) is often considered to be related to thermal volume changes due to magnetic fluctuations^{24,55}. The present investigation allows us to explain the anti-Invar effect of high-temperature γ phase of iron within a simple Heisenberg-like model in terms of magnetic softening of the bulk modulus, without any assumptions about two magnetic states of iron atoms with high and low volumes¹⁷.

Due to the thermal expansion effective exchange parameters increases with the temperature increase,

$$J_0^{ef} = J_0 + \lambda T, \quad (11)$$

with a positive constant $\lambda > 0$. If we substitute this

formula into the mean-field expression for the magnetic susceptibility^{3,25,26},

$$\chi = \frac{m^2}{3(T - 2J_0^{ef}/3)} \quad (12)$$

one can see that corresponding temperature dependence leads to an increase of the effective magnetic moment, $m^2 \rightarrow m^2/(1 - 2\lambda/3)$ and the Curie temperature, $T_C \rightarrow T_C/(1 - 2\lambda/3)$.

To conclude, we have carried out a systematic study of exchange parameters in α - and γ -Fe as functions of the volume and tetragonal deformation. The computational results demonstrate a strong coupling between lattice and magnetic degrees of freedom which should be taken into account in thermodynamic properties of Fe, especially its thermal expansion. Accurate analysis of the magnetic-structure independent contribution E_0 allows us to conclude that a response of fcc and bcc Fe to deformations is mainly controlled by the magnetic exchange.

V. ACKNOWLEDGMENTS

M.I.K. acknowledges financial support from EU-Indian scientific collaboration program, project MONAMI. We thank Igor Abrikosov for critical fruitful discussions. The calculations were partly performed on the supercomputer at NRC ‘‘Kurchatov Institute’’.

-
- ¹ *Physical Metallurgy*, edited by R.W. Cahn and P. Haasen, (North Holland, Amsterdam, 1996).
- ² C. Herring, In: *Magnetism*, ed. by G.T. Rado and H. Suhl (New York, Academic press, 1966, vol 4).
- ³ S.V. Vonsovsky, *Magnetism* (Wiley, New York, 1974).
- ⁴ S.V. Vonsovsky, M.I. Katsnelson, and A.V. Trefilov *Phys. Met. Metallography* **76**, 247 (1993); **76**, 343 (1993).
- ⁵ A.I. Lichtenstein, M.I. Katsnelson, and G. Kotliar, *Phys. Rev. Lett.* **87**, 067205 (2001).
- ⁶ C. Carbone, M. Veronese, P. Moras, S. Gardonio, C. Grazioli, P.H. Zhou, O. Rader, A. Varykhalov, C. Krull, T. Balashov, A. Mugarza, P. Gambardella, S. Lebegue, O. Eriksson, M.I. Katsnelson, and A.I. Lichtenstein *Phys. Rev. Lett.* **104**, 117601 (2010).
- ⁷ L. Kaufman and M. Cohen, *Prog. Metal Phys.* **7**, 165 (1958).
- ⁸ H. Hasegawa, and D.G. Pettifor, *Phys. Rev. Lett.* **50**, 130 (1983).
- ⁹ G.L. Krasko and G.B. Olson, *Phys. Rev. B* **40**, 11536 (1989).
- ¹⁰ D.W. Boukhvalov, Yu.N. Gornostyrev, M.I. Katsnelson, and A.I. Lichtenstein, *Phys. Rev. Lett.* **99**, 247205 (2007).
- ¹¹ V.P. Antropov, M.I. Katsnelson, M. van Schilf-gaarde, B.N. Harmon, *Phys. Rev. Letters* **75**, 729 (1995); V.P. Antropov, M.I. Katsnelson, B.N. Harmon, M. van Schilf-gaarde, D. Kusnezov, *Phys. Rev. B* **54**, 1019 (1996).
- ¹² P. James, O. Eriksson, B. Johansson, and I.A. Abrikosov, *Phys. Rev. B* **59**, 419 (1999).
- ¹³ M. Marsman and J. Hafner, *Phys. Rev. B* **66**, 224409 (2002).
- ¹⁴ I.A. Abrikosov, A.E. Kissavos, F. Liot, B. Alling, S.I. Simak, O. Peil, and A.V. Ruban, *Phys Rev B*, **76**, 014434 (2007).
- ¹⁵ R.F. Sabiryanov, S.K. Bose, and O.N. Mryasov, *Phys. Rev. B* **51**, 8958 (1995).
- ¹⁶ A.V. Ruban, M.I. Katsnelson, W. Olovsson, S.I. Simak, I.A. Abrikosov, *Phys. Rev. B* **71**, 054402 (2005).
- ¹⁷ E.F. Wasserman, in *Ferromagnetic Materials*, edited by K.H.J. Buschow and E.P. Wohlfarth (North-Holland, Amsterdam, 1990), V. 5, p. 237.
- ¹⁸ S.V. Okatov, A.R. Kuznetsov, Yu.N. Gornostyrev, V.N. Urtsev, and M.I. Katsnelson, *Phys. Rev. B* **79**, 094111 (2009).
- ¹⁹ S. Khmelevskiy, and P. Mohn, *Phys. Rev. B* **69** 140404(R) (2004).
- ²⁰ Y. Tsunoda, N. Orishi, and N. Kunitomi, *J. Phys. Soc. Japan* **53**, 359 (1984).
- ²¹ S.V. Sudareva, V.A. Rassokhin, and A.F. Prekul, *Phys. stat. sol (a)* **76**, 101 (1983).

- ²² K. Ullakko, J.K. Huang, C. Kantner, R.C. OHandley, and V.V. Kokorin, *Appl. Phys. Lett.* **69**, 1966 (1996).
- ²³ Y. Tsunoda, L. Hao, S. Shimomura, F. Ye, J.L. Robertson, and J. Fernandez-Baca, *Phys. Rev B* **78**, 094105 (2008).
- ²⁴ M. Acet, H. Zähres, and E.F. Wassermann, W. Pepperhoff, *Phys. Rev. B* **49**, 6012 (1994).
- ²⁵ A.I. Liechtenstein, M.I. Katsnelson, and V.A. Gubanov, *J. Phys. F* **14**, L125 (1984); *Solid State Commun.* **54**, 327 (1985)
- ²⁶ A.I. Liechtenstein, M.I. Katsnelson, V.P. Antropov, and V.A. Gubanov, *J. Magn. Magn. Mater.* **67**, 65 (1987).
- ²⁷ M. Uhl and J. Kübler, *J. Phys.: Condens. Matter* **9**, 7885 (1997).
- ²⁸ L.M. Sandratskii, *Adv. Phys.* **47**, 91 (1998).
- ²⁹ M.I. Katsnelson and A.I. Lichtenstein, *J. Phys: Condens. Matter* **16**, 7439 (2004).
- ³⁰ S.A. Turzhevskii, A.I. Lichtenstein, and M.I. Katsnelson, *Fizika Tverdogo Tela* **32**, 1952 (1990).
- ³¹ G. Kresse and J. Furthmüller, *Phys. Rev. B* **54**, 11169 (1996).
- ³² G. Kresse and J. Hafner, *Journal Phys. Condensed Matter*, **6**, 8245 (1994).
- ³³ G. Kresse and D. Joubert, *Phys. Rev. B* **59**, 1758 (1999).
- ³⁴ P.E. Blöchl, *Phys. Rev. B* **50**, 17953 (1994).
- ³⁵ J.P. Perdew, J.A. Chevary, S.H. Vosko, K.A. Jackson, M.R. Pederson, D.J. Singh, and C. Fiolhais, *Phys. Rev. B* **46**, 6671 (1992); **48**, 4978 (1993).
- ³⁶ S.H. Vosko, L. Wilk, M. Nusair, *Can. J. Phys.* **58**, 1200 (1980).
- ³⁷ H.J. Monkhorst and J.D. Park, *Phys. Rev. B* **13**, 5188 (1976).
- ³⁸ S. Shallcross, A.E. Kissavos, S. Sharma, and V. Meded, *Phys. Rev. B* **73**, 104443 (2006).
- ³⁹ O.N. Mryasov, V.A. Gubanov, and A.I. Liechtenstein, *Phys.Rev. B* **45**, 12330 (1992).
- ⁴⁰ S. Morán, C. Ederer, and M. Fähnle, *Phys. Rev. B* **67**, 012407 (2003).
- ⁴¹ M. Pajda, J. Kudrnovský, I. Turek, V. Drchal, and P. Bruno, *Phys. Rev. B* **64**, 174402 (2001).
- ⁴² M. van Schilfgaarde and V.P. Antropov, *J. Appl. Phys.*, **85**, 4827 (1999).
- ⁴³ V.P. Antropov, B.N. Harmon, and A.N. Smirnov, *J. Magn. Magn. Mater.* **200**, 148 (1999).
- ⁴⁴ D. Špišák, J. Hafner, *J. Magn. Magn. Mater.* **168**, 257 (1997).
- ⁴⁵ S. Frota-Pessôa, R.B. Muniz, J. Kudrnovský, *Phys. Rev. B* **62**, 5293 (2000).
- ⁴⁶ N.M. Rosengaard and B. Johansson, *Phys. Rev. B* **55**, 14975 (1997).
- ⁴⁷ V.M. García-Suárez, C.M. Newman, C.J. Lambert at al, *Eur. Phys. J. B* **40**, p.371 (2004).
- ⁴⁸ H.C. Herper, E. Hoffmann, and P. Entel, *Phys. Rev. B* **60**, 3839 (1999).
- ⁴⁹ M. Friák, M. Šob, V. Vitek, *Phys. Rev. B* **63**, 052405 (2001).
- ⁵⁰ Y. Tsunoda, N. Kunitomi and R.M. Nicklow, *J. Phys. F: Met. Phys.* **17**, 2447 (1987).
- ⁵¹ L. Tsetseris, *Phys. Rev. B* **72**, 012411 (2005).
- ⁵² F. Birch, *Phys. Rev.* **71**, 809 (1947).
- ⁵³ C. Kittel, *Introduction to Solid State Physics* (Wiley, New York, 1958).
- ⁵⁴ M. Hayase, M. Shiga, and J. Nakamura, *J. Phys. Soc. Japan* **30**, 729 (1971).
- ⁵⁵ E.F. Wasserman and P. Entel, *J. de Physique IV* **C8**, 287 (1995).